



Optical anisotropy and electronic structures of CdMoO₄ and CdWO₄ crystals: Polarized reflection measurements, x-ray photoelectron spectroscopy, and electronic structure calculations

Masami Fujita

Japan Coast Guard Academy, Wakaba, Kure 737-8512, Japan

Minoru Itoh, Tsuyoshi Katagiri, and Daisuke Iri

Department of Electrical and Electronic Engineering, Shinshu University, Nagano 380-8553, Japan

Mamoru Kitaura

Fukui National College of Technology, Sabae 916-8507, Japan

Vitalii B. Mikhailik

Physics Department, University of Oxford, Keble Road, Oxford OX1 3RH, United Kingdom

(Received 13 January 2008; published 17 April 2008)

The polarized reflectivity spectra of CdMoO₄ single crystals with a scheelite structure and of CdWO₄ with a wolframite structure are measured in the 3–30 eV range by using synchrotron radiation. The spectra of optical constants for the crystallographic axes are derived by a Kramers–Kronig analysis. X-ray photoelectron spectroscopy (XPS) and the calculation of the electronic structure by using a discrete variational $X\alpha$ method are performed for CdMoO₄. The calculation shows that the Cd $4d$ state is localized at the bottom region of the O $2p$ valence band, and the Cd $5s$ state has a significant contribution to the bottom of the conduction band, composed of the Mo $4d$ state. The XPS spectrum of CdMoO₄ resembles that of CdWO₄. Unlike the XPS spectrum, the optical spectra of CdMoO₄ resemble those of scheelite CaMoO₄ rather than CdWO₄. An excitonic transition is observed as a weak shoulderlike structure in CdWO₄, while it is not appreciable in CdMoO₄. These experimental results are discussed in comparison with the theoretical calculation of electronic structures. The remarkable anisotropy of the optical spectra in CdMoO₄ is explained by taking into account the presence of the Cd $5s$ state at the bottom of the conduction band. The dichroism of CdWO₄ is discussed in terms of the chain structure of WO₆⁶⁻ octahedra in wolframite crystals. The present study indicates that the Cd metal states play a crucial role in the optical properties near the fundamental absorption edge in both CdMoO₄ and CdWO₄.

DOI: [10.1103/PhysRevB.77.155118](https://doi.org/10.1103/PhysRevB.77.155118)

PACS number(s): 78.20.Ci, 71.35.Cc, 78.40.-q

I. INTRODUCTION

The optical and luminescence properties of metal tungstates and molybdates have been given great attention for decades, as these compounds are widely used as scintillating detectors in high-energy particle physics,^{1,2} rare event searches,³ and medical diagnoses.^{4,5} They are also very interesting from the viewpoint of fundamental science, because the self-trapped exciton states exhibit an intrinsic instability due to the Jahn–Teller effect.^{6,7} Metal tungstates and molybdates usually crystallize in either scheelite or wolframite structure.^{8–11} The scheelite structure naturally forms in the materials with larger metal ions such as Pb, Ca, and Ba, while the wolframite structure is generally a more closely packed structure that can be found in the materials with small metal ions such as Zn, Mn, or Fe. Among these compounds, CdMoO₄ and CdWO₄ are of particular interest. Though both have the same metal element as a constituent, the former crystallizes in the scheelite structure and the latter in the wolframite structure.

The scheelite structure belongs to the space group $I4_1/a$. The crystal is tetragonal and therefore optically uniaxial. The optical axis is parallel to the crystallographic c axis, while the a and b axes are equivalent to each other. In CdMoO₄ crystal, each Mo site is surrounded by four equivalent O sites to form MoO₄²⁻ oxyanion molecule of approximately tetra-

hedral symmetry. On the other hand, the wolframite structure is in the monoclinic class and belongs to the $P2/c$ space group. The crystal is optically biaxial, with the b axis as a unique principal axis of the dielectric tensor. The crystallographic a and c axes in the plane perpendicular to the b axis do not intersect at a right angle, in general, and do not necessarily coincide with the principal axes of the dielectric tensor nor the optical axes. In CdWO₄ crystal, each W site is surrounded by six O sites in approximately octahedral coordination.⁹ The WO₆⁶⁻ octahedra form a chain by edge sharing. It should be noted that although the same terms, a , b , and c axes, are used for the scheelite and wolframite crystals in this paper, their meanings are different because of the difference in the crystal structure.

For a decade, we have been carrying out a systematic research on the optical properties of oriented tungstate and molybdate crystals, paying special attention to the optical anisotropy, in order to clarify their electronic structures.^{12–14} A marked dichroism of the exciton band with some fine structures has been found in PbWO₄, which can be explained in terms of the cationic transition in Pb²⁺ ion placed in the uniaxial crystal field.¹³ This result indicates a substantial contribution of the Pb state to the top of the valence band and the bottom of the conduction band in PbWO₄. From a comparative study of CaMoO₄ and CaWO₄,¹⁴ we confirmed that the lowest absorption spectra of Ca compounds are as-

cribed to the transitions from the O 2*p* valence band to the Mo 4*d* or W 5*d* conduction band. This result indicates that the contribution of Ca state to the lowest absorption band is negligible since the unoccupied Ca 3*d* state is located higher in the energy region than the Mo 4*d* (W 5*d*) conduction-band bottom. From a more detailed analysis, it was revealed that the lowest absorption band has an anisotropic composite nature in both CaMoO₄ and CaWO₄, which is explained on the basis of a picture of the intramolecular transition in an oxyanion complex.

The electronic structures of Pb, Ca, and Cd tungstates and molybdates have been calculated by a linearized-augmented-plane wave (LAPW) method.^{15,16} Very recently, a relativistic molecular orbital calculation has been performed for Pb, Ca, Ba, Cd, and Zn tungstates by using a discrete variational $X\alpha$ (DV- $X\alpha$) method.¹⁷ The DV- $X\alpha$ calculations show that the electronic structures of tungstates are classified into three categories on the basis of the contribution of the metal states to the top of the valence band and/or the bottom of the conduction band. In PbWO₄, the Pb state contributes to a large extent to both the conduction-band bottom and the valence-band top. On the other hand, there are negligible contributions of the metal states to the top of the valence band and the bottom of the conduction band in CaWO₄ and BaWO₄. In the cases of CdWO₄ and ZnWO₄, a significant contribution of the metal states is found at the bottom of the conduction band, while their contributions are negligible on the top of the valence band. The calculation results explain well the experimental spectra in the fundamental absorption-edge region in PbWO₄,¹³ CaWO₄,¹⁴ and ZnWO₄.¹⁸ Only recently, x-ray photoelectron spectroscopy (XPS) studies have been carried out for these tungstates to clarify the electronic structures of the valence bands and outermost-core levels.¹⁷ No XPS spectra have been reported for molybdates.

It is particularly interesting to compare the optical and XPS spectra of CdMoO₄ with those of CdWO₄, because they have the same metal cation but form different crystal structures. This comparison is expected to provide us with useful information for understanding the electronic structures of tungstate and molybdate compounds. Furthermore, as the unoccupied Cd 5*s* state is expected to be located in the lower energy part of the Mo 4*d* or W 5*d* conduction band when compared with Ca compounds, one expects a noticeable contribution of the metal state to the optical properties of Cd compounds. The reflection spectrum of CdWO₄ has been measured earlier by Kolobanov *et al.*¹⁹ and Nagirnyi *et al.*,^{20,21} and that of CdMoO₄ has been measured recently by Mikhailik *et al.*²² No optical constants, however, have been derived from these data.

In the present study, the polarized reflectivity spectra of oriented CdMoO₄ and CdWO₄ crystals are measured using synchrotron radiation as a light source. The optical constants for the directions of crystallographic axes are obtained by a Kramers–Kronig analysis. The XPS spectrum of CdMoO₄ is also measured and compared with that of CdWO₄. A theoretical calculation of the electronic structure of CdMoO₄ is carried out using the DV- $X\alpha$ method. The optical properties and electronic structures of CdMoO₄ and CdWO₄ are discussed on the basis of present results as well as our previous studies.^{13,14,17,18}

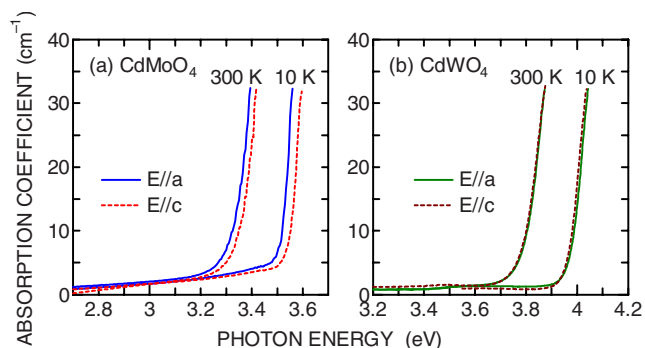


FIG. 1. (Color online) Absorption spectra of (a) CdMoO₄ and (b) CdWO₄ for $E\parallel a$ and $E\parallel c$ at 10 and 300 K.

II. EXPERIMENT

Single crystals of CdMoO₄ and CdWO₄ were grown by the Czochralski technique. The crystal orientation was confirmed by x-ray diffraction. For reflection measurements, the surface of the *ac* plane of the CdMoO₄ crystal was mechanically polished, while the *ac* plane of the CdWO₄ crystal was obtained by cleavage. Optical measurements were carried out at the beamline BL-1B of UVSOR facility at the Institute for Molecular Science, Okazaki. The light beam was monochromatized through a 1 m Seya–Namioka monochromator, with a typical resolution of 0.5 nm, and the reflected light was measured under near-normal incidence ($\sim 10^\circ$) up to 30 eV. The electric vector of the incident light was parallel to the *a* axis ($E\parallel a$) or *c* axis ($E\parallel c$) of the crystals. The samples were mounted on the copper holder of a He-flow cryostat. The base pressure of the sample chamber was kept at about 1.0×10^{-6} Pa. Absorption spectra near the fundamental absorption edge were also measured.

XPS spectra were obtained using an ESCA spectrometer (ULVAC-PHI 5600). The measurements were performed for a freshly cleaved sample surface. Monochromatized x-ray ($K\alpha$: 1486.6 eV) from an Al anode was used for excitation. An electron flood gun was employed to compensate for the sample charging under x-ray irradiation. The overall resolution was about 0.5 eV under our experimental conditions. The base pressure in the sample chamber was less than 6.0×10^{-8} Pa during the measurements.

III. RESULTS

The absorption spectra of CdMoO₄ and CdWO₄ crystals measured at 10 and 300 K are shown in Figs. 1(a) and 1(b), respectively. The absorption edge of both materials is slightly dependent on the light polarization orientation. The excitation threshold for the intrinsic luminescence of CdMoO₄ (Ref. 23) and CdWO₄ (Ref. 21) at low temperatures coincides with the corresponding onset of the absorption spectra at 10 K in Figs. 1(a) and 1(b).

In reflection measurements, multiple reflection was observed in the spectral region below the fundamental absorption edge. In order to avoid this effect, the reflectivity *R* in this region was extrapolated using the data on the dispersion of refractive index *n* and the relation $R = (n-1)^2 / (n+1)^2$. For

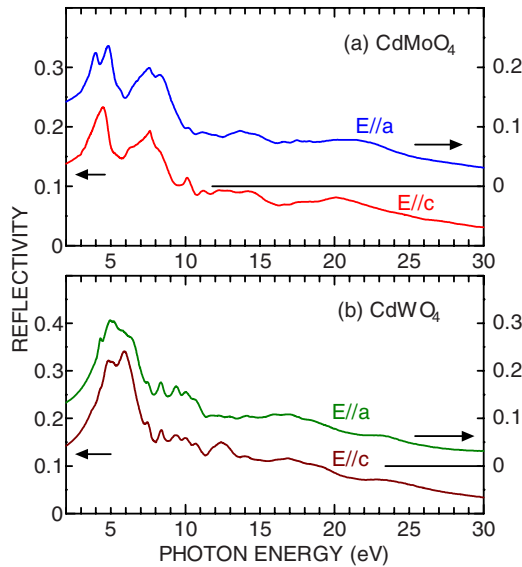


FIG. 2. (Color online) Reflectivity spectra of (a) CdMoO₄ and (b) CdWO₄ for $\mathbf{E}\parallel\mathbf{a}$ and $\mathbf{E}\parallel\mathbf{c}$ at 10 K.

CdMoO₄, the refractive indices of the ordinary and extraordinary rays at room temperature from Ref. 24 were used to calculate the reflectivity for two polarizations. In the case of CdWO₄, the values of reflectivity for $\mathbf{E}\parallel\mathbf{a}$ and $\mathbf{E}\parallel\mathbf{c}$ were calculated using the refractive indices measured for the optical Y axis and Z axis at room temperature, respectively.²⁵ Although the $Y(Z)$ axis makes an angle of 15° (13.5°) to the $a(c)$ axis, the values of the refractive indices for the crystallographic a and c axes are approximately the same as those of the Y and Z axes. Each reflectivity spectrum measured above the absorption edge was connected to the calculated spectrum below the edge by multiplication with a constant factor. The reflectivity spectra of CdMoO₄ and CdWO₄ thus obtained are shown in Figs. 2(a) and 2(b), respectively.

For CdMoO₄ in Fig. 2(a), a remarkable dichroism is seen around 4–6 eV. Two distinct peaks and a weak peak are observed for $\mathbf{E}\parallel\mathbf{a}$, while a peak is observed for $\mathbf{E}\parallel\mathbf{c}$ in this region. In the 6–9 eV region, a broad band with two peaks at 7.6 and 8.4 eV is seen for both polarizations. Weak structures without a clear dichroism appear above 10 eV. The reflectivity spectrum of CdMoO₄ previously reported²² is similar to that for $\mathbf{E}\parallel\mathbf{a}$ in Fig. 2(a).

For CdWO₄ in Fig. 2(b), a broad structured band is seen in the 4–7 eV region. The structure of this band exhibits polarization dependence. A small peak or shoulder is found at 4.3 eV for both polarizations. A characteristic structure composed of several peaks appears in the 7–11 eV region. No distinct features are observed above 11 eV except for a broad band peaking at 12 eV for $\mathbf{E}\parallel\mathbf{c}$. The reflectivity spectra of CdWO₄ have been reported in Refs. 19–21. The spectrum for $\mathbf{E}\parallel\mathbf{c}$ below 10 eV in Ref. 20 is in general agreement with that for $\mathbf{E}\parallel\mathbf{c}$ in Fig. 2(b). The spectrum for $\mathbf{E}\perp\mathbf{c}$ in Ref. 19, on the other hand, resembles our spectrum for $\mathbf{E}\parallel\mathbf{c}$ rather than for $\mathbf{E}\parallel\mathbf{a}$.

The dielectric functions of CdMoO₄ and CdWO₄ were calculated using a Kramers–Kronig analysis. Figures 3 and 4 show the real (ϵ_1) and imaginary (ϵ_2) parts of the dielectric

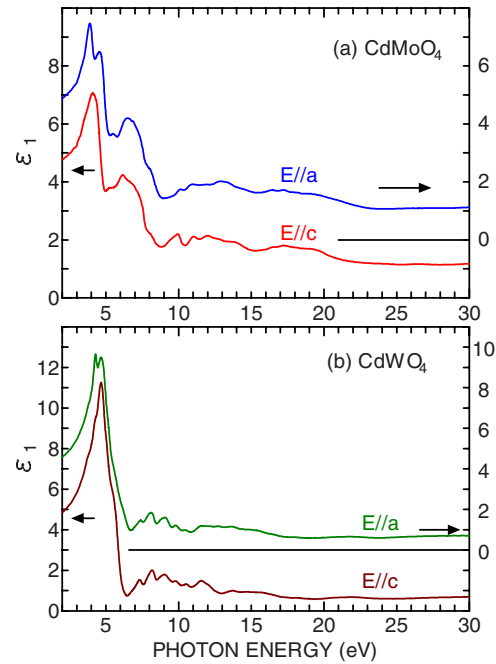


FIG. 3. (Color online) Real part of the dielectric function of (a) CdMoO₄ and (b) CdWO₄ for $\mathbf{E}\parallel\mathbf{a}$ and $\mathbf{E}\parallel\mathbf{c}$ at 10 K.

functions, respectively. The imaginary parts below 14 eV are also presented in an expanded scale in Figs. 5(a) and 5(b). In Fig. 5(a), the spectra of CdMoO₄ are classified into two groups around 5 eV (region I) and 8 eV (region II), respectively. Region I consists of three peaks at 4.1, 4.9, and 5.7 eV for $\mathbf{E}\parallel\mathbf{a}$ and of a peak at 4.6 eV for $\mathbf{E}\parallel\mathbf{c}$. Interestingly, a global feature of the CdMoO₄ spectra is similar to that of the CaMoO₄ spectra previously reported in Ref. 14, rather than the CdWO₄ spectra displayed in Fig. 5(b). The structures in the spectra of CdWO₄ in Fig. 5(b) are also classified into two groups: region I with broad bands and region II with several peaks. The peaks at 5.0, 5.2, 5.8, and 6.4 eV for $\mathbf{E}\parallel\mathbf{a}$, and at 4.9, 5.2, and 5.8 eV for $\mathbf{E}\parallel\mathbf{c}$ are observed in region I.

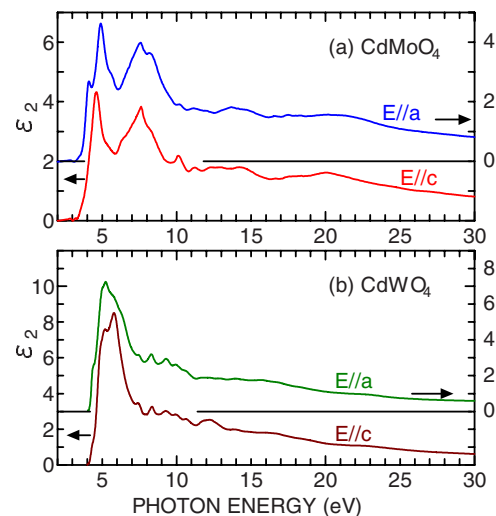


FIG. 4. (Color online) Imaginary part of the dielectric function of (a) CdMoO₄ and (b) CdWO₄ for $\mathbf{E}\parallel\mathbf{a}$ and $\mathbf{E}\parallel\mathbf{c}$ at 10 K.

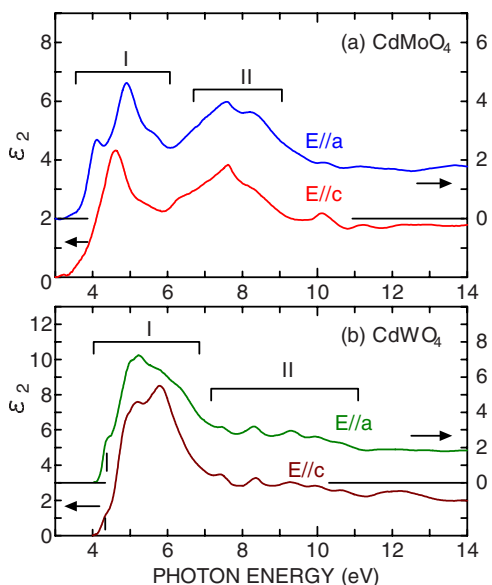


FIG. 5. (Color online) Imaginary part of the dielectric function of (a) CdMoO_4 and (b) CdWO_4 for $\mathbf{E}\parallel\mathbf{a}$ and $\mathbf{E}\parallel\mathbf{c}$ at 10 K below 14 eV in an expanded scale.

The XPS spectrum of CdMoO_4 measured at 300 K is presented in Fig. 6. The binding energy is given relative to the top of the valence band. The valence band has a full base width of about 6 eV. A strong peak at 8.5 eV and a small peak at 19 eV are assigned to the Cd 4d and O 2s core levels, respectively, in analogy to CdWO_4 .¹⁷ In contrast to the optical spectra, the XPS spectrum of scheelite CdMoO_4 exhibits similarity to that of wolframite CdWO_4 and is distinctively different from those of scheelite tungstates such as PbWO_4 , BaWO_4 , and CaWO_4 (see Figs. 6 and 7 in Ref. 17).

IV. ELECTRONIC STRUCTURE OF CdMoO_4 BY THE DV- $X\alpha$ CALCULATION

The electronic structures of metal tungstates have been calculated by the LAPW method^{15,16} and by the DV- $X\alpha$ method.¹⁷ Although there are agreements on many points between both calculations, some noticeable differences were found. The electronic structures of metal molybdates have also been studied by the LAPW method,^{15,16} but not by the DV- $X\alpha$ method. In the present study, the DV- $X\alpha$ calculation

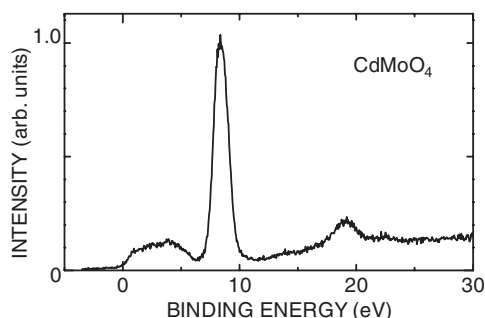


FIG. 6. XPS spectrum of CdMoO_4 at 300 K. The binding energy is given relative to the top of the valence band.

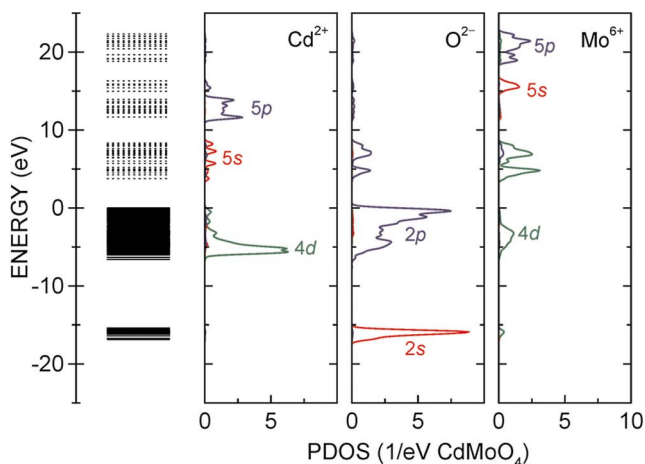


FIG. 7. (Color online) Energy diagram and partial density of states per molecule for CdMoO_4 .

was applied to CdMoO_4 . The calculation method is described in detail in Ref. 26.

As a first step, a simple cluster of $[\text{Cd}(\text{MoO}_4)_4]^{6-}$ was chosen for the calculation without taking into account the Madelung potential (MP). The calculation gave us a good agreement with the XPS data and a reasonable value (4 eV) for the band-gap energy. When the MP was taken into account, however, the Cd 4d state, which lies below the valence-band bottom as evidenced in the XPS spectrum (Fig. 6), was buried into the O 2p valence band. Therefore, a larger cluster of $[\text{Cd}_9\text{Mo}_{10}\text{O}_{68}]^{58-}$ was selected as a next step. The calculation for this cluster including the MP showed that the Cd 4d state is concentrated just below the O 2p valence band. Furthermore, an acceptable value of 3.76 eV for the band-gap energy was received.

The partial density of states (PDOS) obtained for the $[\text{Cd}_9\text{Mo}_{10}\text{O}_{68}]^{58-}$ cluster is displayed in Fig. 7. The valence band is dominated by the O 2p state, exhibiting a marked hybridization with the Mo 4d state in the bottom region. The narrow Cd 4d state is located at about 5.5 eV. The O 2s state appears at 16 eV. The calculated binding energies of the core states are underestimated (2–3 eV) when compared to the experimental result in Fig. 6. Such underestimation is also found in the DV- $X\alpha$ results obtained for tungstates.¹⁷ The lower conduction band is mainly made of the Mo 4d state. A significant difference between the LAPW and DV- $X\alpha$ calculations is in the degree of the contribution of the Cd 5s state to the bottom of the conduction band. The LAPW calculations show that the Mo 4d state is dominant,¹⁶ while the DV- $X\alpha$ results indicate that the contribution of the Cd 5s PDOS is comparable with that of the Mo 4d state. In the DV- $X\alpha$ calculation, the partial contributions of the electronic states of Cd, O, and Mo atoms to the bottom of the conduction band are 43.1%, 4.3%, and 52.6%, respectively. The contributions of these states to the top of the valence band are 5.6%, 93.2%, and 1.2%, respectively. It is worthwhile to note that these values are comparable with those obtained for CdWO_4 .¹⁷

Another difference between the LAPW and DV- $X\alpha$ calculations is observed in the value of the band-gap energy E_g . This difference is more remarkable in scheelite CdMoO_4

than in wolframite CdWO_4 . For CdMoO_4 , the calculated DV- $X\alpha$ value of E_g is 3.76 eV, which is considerably larger than 2.43 eV by the LAPW method.¹⁶ Our value of 3.76 eV is close to the experimental value [4.0 eV (Ref. 23)]. For CdWO_4 , the calculated value (2.76 eV) of E_g by the DV- $X\alpha$ method¹⁷ is comparable with 2.94 eV by the LAPW method.¹⁶ These values are both smaller than the experimental ones [4.5 eV (Ref. 16) or 5.0 eV (Ref. 20)].

V. DISCUSSION

From the present experiment, it is clear that the XPS spectrum of scheelite CdMoO_4 manifests a striking resemblance to that of wolframite CdWO_4 but not to those of other scheelite tungstates. This result indicates that the distribution of the PDOS in the valence band of both materials is similar, despite the difference in the crystal structure. The resemblance of the XPS spectra also supports our theoretical calculation that the Cd 4*d* state is concentrated at the bottom region of the valence band, which is mainly formed by the O 2*p* state in both Cd compounds.

In contrast to the XPS spectra, there is no obvious similarity between the optical spectra of CdMoO_4 and CdWO_4 as shown in Figs. 2–5. The dissimilarity of optical spectra is primarily ascribed to the difference in the conduction-band states, because the valence-band PDOS is highly similar in both materials. It should be noted that the character of the conduction band mainly made of the Mo 4*d* or W 5*d* state is determined by the coordination of O atoms around the Mo or W site. The lower and upper parts of the conduction band are associated with the *e* and t_2 states, respectively, in the scheelite crystals, and vice versa in the wolframite crystals, due to the crystal-field splitting of the Mo 4*d* or W 5*d* state.¹⁶ The optical spectra calculated in Ref. 16 show two groups of structures around 6 and 9 eV for CdMoO_4 , and around 6 and 11 eV for CdWO_4 , that reflects the splitting of the *d* state in the conduction band. These features reproduce the overall structures in Figs. 5(a) and 5(b) if the calculated spectra are shifted to lower energy by 1 eV. The structures in regions I and II of CdMoO_4 in Fig. 5(a) are assigned to the transitions to the lower part of the conduction band with the *e* character, and to the upper part with the t_2 character, respectively. As for CdWO_4 , the broad band in region I and the structure in region II in Fig. 5(b) are ascribed to the transitions to the lower t_2 state and to the upper *e* state in the conduction band, respectively. The calculations of Ref. 16 thus explain well the experimental result that the two groups of structures appear in the optical spectra of both crystals. Although the detailed arguments like those above have not been made, the authors of Refs. 19 and 21 have also ascribed the structures of CdWO_4 in the region below 15 eV to the transitions from the O 2*p* valence band to the W 5*d* conduction band. Nevertheless, further consideration is necessary in order to clarify the origin of each structure and its polarization dependence. In the LAPW calculations of Ref. 16, the contribution of the Cd 5*s* state to the conduction-band bottom is negligibly small, in contrast to our DV- $X\alpha$ calculation. In the following, we will discuss the importance of the Cd metal state for the optical properties near the absorption edge in the materials under investigation.

The experimental values of E_g of CdMoO_4 and CdWO_4 have not been precisely determined. For CdWO_4 , the authors of Ref. 16 obtained $E_g \approx 4.5 \pm 0.2$ eV from the threshold energy of two-photon absorption spectra. On the other hand, the value of 5 eV was obtained from the threshold energy of free carrier creation by a photostimulated luminescence (PSL) experiment.²⁰ In either case, the small peak at 4.3 eV in Fig. 5(b) is located below the band gap and is assigned to the excitonic transition. In the case of CdMoO_4 , we get $E_g \approx 4.0$ eV from the threshold energy of free carrier creation by the PSL experiment.²³ Two-photon experiments have not been performed for CdMoO_4 . If the value of 4.0 eV is correct as E_g , it is natural to suppose that the lowest band at 4.1 eV in Fig. 5(a) results from the joint density of states. In other words, no structure suggestive of exciton transition is observed in CdMoO_4 .

It is worth considering that the exciton structure is seen in wolframite CdWO_4 , but not in scheelite CdMoO_4 . For both materials, the degree of hybridization of the Cd and W (Mo) states is large in the conduction-band bottom, while that of the Cd and O states is negligibly small in the uppermost valence band. In Ref. 14, we pointed out that no structure due to excitonic transition is observed in scheelite CaMoO_4 and CaWO_4 . This result indicates that the intensity of the excitonic transition is very weak for the optical transition from the O 2*p* state to the Mo 4*d* (W 5*d*) state. A similar situation takes place in scheelite CdMoO_4 , although the Mo conduction band is highly hybridized with the Cd state. In the case of CdWO_4 , we suppose that some perturbation such as the crystal field or local lattice deformation exists due to the lower symmetry of the wolframite structure. Because of such perturbation, the Cd 4*d* state will mix with the O 2*p* valence state to form the hybridized Cd 4*d*-O 2*p* state in the upper part of the valence band. If this is the case, the excitonic 4*d*→5*s* transition in Cd^{2+} ions is expected to occur with a small oscillator strength in wolframite CdWO_4 . The parity forbiddenness could be lifted through the mixing with the O 2*p* state. A similar weak cationic exciton transition has been observed in ZnWO_4 with the wolframite structure, as well.¹⁸

We examine the origin of the remarkable dichroism of CdMoO_4 in region I in Fig. 5(a), where three peaks and a single peak are observed for $\mathbf{E}\parallel\mathbf{a}$ and $\mathbf{E}\parallel\mathbf{c}$, respectively. As is shown by the DV- $X\alpha$ calculation, the optical excitation near the absorption edge is regarded as being due to the transition from the O 2*p* valence band to the conduction band composed of the Mo 4*d* state with a considerable contribution of the Cd 5*s* state. We propose an energy-level diagram shown in Fig. 8 to explain the anisotropic optical spectra. In a free MoO_4^{2-} molecule of T_d symmetry, the highest occupied orbital made of the O 2*p* state is of t_1 symmetry, while the lowest and next higher unoccupied orbitals made of the Mo 4*d* state are of *e* and t_2 symmetries, respectively.²⁷ In the scheelite crystal, the molecule is slightly compressed along the *c* axis and the symmetry is lowered to D_{2d} . Because of the surrounding ions, the site symmetry of the oxyanion molecule is further lowered to S_4 . The occupied t_1 state in T_d symmetry splits into the *e* and *a* sublevels in S_4 symmetry, and they form the upper part of the valence band shaded in Fig. 8. The unoccupied *e* and t_2 states split into the

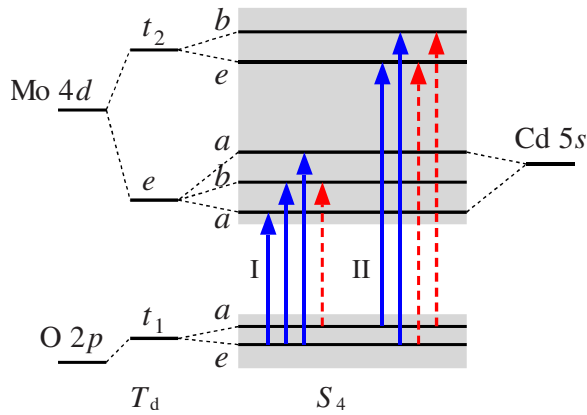


FIG. 8. (Color online) Schematic diagram of the energy levels of CdMoO_4 . The lower and upper shaded boxes indicate the valence band and the conduction band, respectively. The assignment of the transitions for the main structures in optical spectra is also shown by arrows. Solid and broken arrows represent the allowed optical transitions for $\mathbf{E}\parallel\mathbf{a}$ and $\mathbf{E}\parallel\mathbf{c}$, respectively.

a and b sublevels and the e and b sublevels, respectively. The $\text{Cd } 5s$ state forms an energy level of a symmetry, which couples with the a sublevel originating from the e state of $\text{Mo } 4d$. The interaction between the two levels with the same symmetry leads to the energy diagram displayed in Fig. 8. In the S_4 symmetry, the electric dipole transitions are allowed between the states $e \leftrightarrow a, b$ for the polarization $\mathbf{E}\parallel\mathbf{a}$, and $a \leftrightarrow b$ and $e \leftrightarrow e$ for $\mathbf{E}\parallel\mathbf{c}$.²⁸ The solid and broken arrows in Fig. 8 indicate the allowed transitions for $\mathbf{E}\parallel\mathbf{a}$ and $\mathbf{E}\parallel\mathbf{c}$, respectively. Therefore, three optical transitions are expected to occur for $\mathbf{E}\parallel\mathbf{a}$ and one transition for $\mathbf{E}\parallel\mathbf{c}$ in region I. This expectation is in good agreement with the experimental result.

The splitting of the t_1 state at the top of the valence band in the diagram of Fig. 8 is estimated to be 0.30 ± 0.05 eV from the separation between the second peak for $\mathbf{E}\parallel\mathbf{a}$ and the lowest peak for $\mathbf{E}\parallel\mathbf{c}$ in Fig. 5(a). The splitting of the three sublevels at the bottom of the conduction band is evaluated from the separations of the three peaks for $\mathbf{E}\parallel\mathbf{a}$; the lowest a sublevel and the next higher b sublevel split by 0.80 ± 0.05 eV, and the b sublevel and the upper a sublevel split by 0.75 ± 0.05 eV. The splitting of the t_1 state of $\text{O } 2p$ at the valence-band top in CdMoO_4 is comparable with that of CaMoO_4 (0.27 ± 0.05 eV).¹⁴ On the other hand, the splitting between the lowest a sublevel and the next higher b sublevel in the conduction-band bottom of CdMoO_4 is about two times larger than that of CaMoO_4 (0.36 ± 0.05 eV). We suppose that the repulsion of the two a sublevels due to the interaction between the states with the same symmetry results in the larger splitting in CdMoO_4 .

The two peaks at 7.6 and 8.4 eV observed for both polarizations in region II in Fig. 5(a) are tentatively assigned to the transitions to the e and b sublevels, respectively, derived from the t_2 state of $\text{Mo } 4d$, as shown in Fig. 8. This assignment, however, conflicts with the observation that the position of each peak is only slightly dependent on the polarization, because the energy separation of 0.3 eV between the peak positions for $\mathbf{E}\parallel\mathbf{a}$ and $\mathbf{E}\parallel\mathbf{c}$ is expected due to the split-

ting of the t_1 state at the valence-band top. The overlap of the optical transitions from the lower portion of the valence band may be responsible for this discrepancy.

As for the spectra of CdWO_4 in Fig. 5(b), it is noted that the structures on the broad band in region I exhibit distinct dichroism, while the peaks in region II are hardly dependent on the polarization. In the case of CdWO_4 , the splitting of energy levels is very complicated because of the low symmetry of the wolframite structure. Moreover, optical measurements for polarizations $\mathbf{E}\parallel\mathbf{a}$ and $\mathbf{E}\parallel\mathbf{c}$ do not provide independent information on the symmetry of the electronic states, since the selection rule for the transitions for both polarizations are the same in the wolframite structure. Therefore, it is not suitable to discuss the dichroism in Fig. 5(b) by using a group-theoretical approach. Here, we make a speculation on the optical transitions in CdWO_4 , paying attention to the crystal structure in which the WO_6^{6-} octahedra form chains along the c axis.⁹ It is supposed that the intensity of the optical transition from the O site in the chain to the Cd site outside of the chain highly depends on the direction of the polarization with respect to the chain axis (i.e., c axis), while the intensity of the transition from the O site to the W site in a WO_6^{6-} octahedron weakly depends on the polarization. If this supposition is correct, the structures exhibiting the dichroism on the broad band in region I in Fig. 5(b) can be interpreted as due to the transitions from the $\text{O } 2p$ state to the $\text{Cd } 5s$ state, which hybridizes with the $\text{W } 5d$ conduction state. In other words, the $\text{Cd } 5s$ state contributes to a certain extent to the lower portion of the conduction band in CdWO_4 , as in the case of CdMoO_4 .

VI. SUMMARY

We measured the polarized reflectivity spectra of oriented CdMoO_4 and CdWO_4 crystals and derived the spectra of the optical constants for the crystallographic axis directions. A remarkable dichroism was observed near the absorption edge in both crystals. The measurement of XPS spectrum and the DV- $X\alpha$ calculation of the energy band structure were carried out for CdMoO_4 . The theoretical calculation highlighted the contribution of Cd states to the lower part of the $\text{O } 2p$ valence band and to the bottom of the $\text{Mo } 4d$ conduction band. The XPS spectrum of CdMoO_4 exhibited a notable resemblance to that of CdWO_4 , indicating the close similarity of the valence-band states of both materials. On the other hand, no obvious similarity was observed between the optical spectra of CdMoO_4 and CdWO_4 . This dissimilarity was ascribed to the difference in the conduction band of both materials due to the difference in crystal structure. The appearance of the cationic exciton transition in CdWO_4 was explained in terms of the mixing of the $\text{Cd } 4d$ state with the $\text{O } 2p$ valence state. A remarkable polarization dependence of the structures in the optical spectra of CdMoO_4 was discussed by taking into account the splitting of the $\text{O } 2p$ valence state and of the $\text{Mo } 4d$ conduction state hybridized with the $\text{Cd } 5s$ state under S_4 symmetry in the scheelite structure. A speculation on

the dichroism near the absorption edge of CdWO₄ was made based on the chain structure of the WO₆⁶⁻ octahedra in wolframite crystals. The results of the present study demonstrate that the Cd metal state plays a crucial role in the optical properties in the fundamental absorption-edge region of CdMoO₄ and CdWO₄, which is consistent with the DV-*X*_α calculation, but not with the previous LAPW calculation.

ACKNOWLEDGMENTS

The authors would like to express their sincere thanks to Y. Usuki for providing the single crystals used in the present experiment and to M. Narukawa for assistance in the DV-*X*_α calculations. This work was supported by the Joint Studies Program of the Institute for Molecular Science.

-
- ¹M. Kobayashi, M. Ishii, Y. Usuki, and H. Yahagi, Nucl. Instrum. Methods Phys. Res. A **333**, 429 (1993).
- ²P. Lecoq, I. Dafinei, E. Auffray, M. Schneegans, M. V. Korzhik, O. V. Missevitch, V. B. Pavlenko, A. A. Fedorov, A. N. Annenkov, V. L. Kostylev, and V. D. Ligun, Nucl. Instrum. Methods Phys. Res. A **365**, 291 (1995).
- ³V. B. Mikhailik and H. Kraus, J. Phys. D **39**, 1181 (2006).
- ⁴W. W. Moses, in *Proceedings of the Fifth International Conference on Inorganic Scintillators and Their Applications*, edited by V. Mikhailin (Moscow State University, Moscow, 2000), p. 11.
- ⁵M. Kobayashi, Y. Usuki, M. Ishii, M. Itoh, and M. Nikl, Nucl. Instrum. Methods Phys. Res. A **540**, 381 (2005).
- ⁶M. Bacci, S. Porcinai, E. Mihóková, M. Nikl, and K. Polák, Phys. Rev. B **64**, 104302 (2001).
- ⁷M. Itoh and T. Sakurai, Phys. Rev. B **73**, 235106 (2006).
- ⁸R. W. G. Wyckoff, *Crystal Structures*, 2nd ed. (Wiley, New York, 1965), Vol. 3, Chap. VIII.
- ⁹M. Daturi, M. M. Borel, A. Leclaire, L. Savary, G. Costentin, J. C. Lavalley, and B. Raveau, J. Chim. Phys. Phys.-Chim. Biol. **93**, 2043 (1996).
- ¹⁰P. F. Schofield, K. S. Knight, S. A. T. Redfern, and G. Cressey, Acta Crystallogr., Sect. B: Struct. Sci. **B53**, 102 (1997).
- ¹¹H. Kraus, V. B. Mikhailik, L. Vasylechko, D. Day, K. B. Hutton, J. Telfer, and Yu. Prots, Phys. Status Solidi A **204**, 730 (2007).
- ¹²M. Itoh and M. Fujita, Phys. Rev. B **62**, 12825 (2000).
- ¹³M. Fujita, M. Itoh, M. Horimoto, and H. Yokota, Phys. Rev. B **65**, 195105 (2002).
- ¹⁴M. Fujita, M. Itoh, S. Takagi, T. Shimizu, and N. Fujita, Phys. Status Solidi B **243**, 1898 (2006).
- ¹⁵Y. Zhang, N. A. W. Holzwarth, and R. T. Williams, Phys. Rev. B **57**, 12738 (1998).
- ¹⁶Y. Abraham, N. A. W. Holzwarth, and R. T. Williams, Phys. Rev. B **62**, 1733 (2000).
- ¹⁷M. Itoh, N. Fujita, and Y. Inabe, J. Phys. Soc. Jpn. **75**, 084705 (2006).
- ¹⁸M. Itoh, T. Katagiri, T. Aoki, and M. Fujita, Radiat. Meas. **42**, 545 (2007).
- ¹⁹V. N. Kolobanov, I. A. Kamenskikh, V. V. Mikhailin, I. N. Shpinkov, D. A. Spassky, B. I. Zadneprovsky, L. I. Potkin, and G. Zimmerer, Nucl. Instrum. Methods Phys. Res. A **486**, 496 (2002).
- ²⁰V. Nagirnyi, E. Feldbach, L. Jönsson, M. Kirm, A. Kotlov, A. Lushchik, V. A. Nefedov, and B. I. Zadneprovski, Nucl. Instrum. Methods Phys. Res. A **486**, 395 (2002).
- ²¹V. Nagirnyi, M. Kirm, A. Kotlov, A. Lushchik, and L. Jönsson, J. Lumin. **102–103**, 597 (2003).
- ²²V. B. Mikhailik, H. Kraus, D. Wahl, and M. S. Mykhaylyk, Phys. Status Solidi B **242**, R17 (2005).
- ²³V. Nagirnyi, P. Dorenbos, E. Feldbach, L. Jönsson, M. Kerikmäe, M. Kirm, E. van der Kolk, A. Kotlov, H. Kraus, A. Lushchik, V. Mikhailik, R. Sarakvasha, and A. Watterich, in *Proceedings of the 8th International Conference on Inorganic Scintillators and Their Use in Scientific and Industrial Applications*, Alushta, Ukraine, 19–23 September 2005, edited by A. Gektin and B. Grinyov (ISMA, Kharkiv, 2006), p. 36.
- ²⁴G. F. Bakhshieva and A. M. Morozov, Sov. J. Opt. Technol. **44**, 542 (1977).
- ²⁵H. Lotem and Z. Burshtein, Opt. Lett. **12**, 561 (1987).
- ²⁶H. Adachi, M. Tsukada, and C. Satoko, J. Phys. Soc. Jpn. **45**, 875 (1978).
- ²⁷R. Kebabcioglu and A. Müller, Chem. Phys. Lett. **8**, 59 (1971).
- ²⁸G. F. Koster, J. O. Dimmock, R. G. Wheeler, and H. Statz, in *Properties of the Thirty-Two Point Groups* (MIT, Cambridge, MA, 1963), p. 40.